Bi-Component Ultra-Short Echo Time T2* Analysis for Assessment of Patients with Patellar Tendinopathy

Richard Kijowski, M.D.[1,3], **John J. Wilson, M.D.**[2], and **Fang Liu, Ph.D.**[1]

[1]Department of Radiology, University of Wisconsin School of Medicine and Public Health, Madison, Wisconsin

[2]Department of Orthopedics and Rehabilitation, University of Wisconsin School of Medicine and Public Health, Madison, Wisconsin

Abstract

Purpose—To compare bi-component ultra-short echo time (UTE) T2* parameters of patellar tendon between healthy volunteers and patients with patellar tendinopathy.

Methods—This study was performed with Institutional Review Board approval and with all subjects signing informed consent. A UTE-T2* mapping sequence was performed at 3.0T on the knees of 10 healthy volunteers and in 11 patients with patellar tendinopathy. The UTE-T2* relaxation times of the fast relaxing macromolecular bound water component ($T2*_F$) and the slow relaxing bulk water component ($T2*_S$) and the fraction of the fast relaxing macromolecular bound water component (F_F) of patellar tendon were measured in all subjects. Wilcoxon rank-sum tests were used to compare UTE-T2* parameters between healthy volunteers and patients with patellar tendinopathy.

Results—Mean $T2*_F$, $T2*_S$, and F_F of the patellar tendon was 1.5ms, 23.1ms, and 79.5% respectively for healthy volunteers and 1.9ms, 22.3ms, and 75.5% respectively for patients with patellar tendinopathy. There were statistically significant differences between groups of subjects for $T2*_F$, (p=0.01) and F_F (p=0.007) but not $T2*_S$ (p=0.10) of the patellar tendon.

Conclusion—Patients with patellar tendinopathy had significantly higher $T2*_F$ and significantly lower F_F of patellar tendon than healthy volunteers which suggests that bi-component UTE-T2* parameters can detect changes in the composition and microstructure of degenerative tendon.

Keywords

Tendon; T2 Relaxation Time; Bi-component; Patella; Ultra-Short Echo Time

INTRODUCTION

Musculoskeletal tissues with an abundant content of highly organized collagen fibers, such as tendon, appear dark when using conventional magnetic resonance imaging (MRI)

[3]Corresponding Author: Richard Kijowski, M.D., Department of Radiology, University of Wisconsin School of Medicine and Public Health, Clinical Science Center- E3/311, 600 Highland Avenue, Madison, Wisconsin 53792-3252, Phone: 608-265-3247, FAX: 608-263-5112, rkijowski@uwhealth.org.

methods due to their extremely rapid signal decay. Ultra-short echo time (UTE) techniques have recently been developed to capture the rapidly decaying signal within musculoskeletal tissues [1]. By acquiring multiple echoes as short as 0.008ms, these techniques can be used to calculate ultra-short echo time T2* (UTE-T2*) relaxation time of tendon [2–7]. Previous studies have documented changes in the UTE-T2* relaxation time of tendon due to cyclic loading [2, 3], various tissue preservation methods [4, 5], strenuous physical activity [6], and pathologic degeneration [7]. However, changes in UTE-T2* relaxation time of tendon are nonspecific and can be potentially caused by multiple factors associated with tendon degeneration including changes in hydration, macromolecular content, and disruption of the collagen fiber network [8].

Bi-component UTE-T2* mapping techniques can potentially improve the sensitivity and specificity of UTE-T2* analysis by assessing the individual water components of tendon. Bi-component UTE-T2* mapping techniques have detected two distinct T2* components within tendon representing fast relaxing water bound to the highly organized collagen fibers and slow relaxing bulk water with T2* relaxation times ranging between 0.3ms and 1.3ms for the short component and 8.2ms and 20.4ms for the long component [3, 9–12]. However, few studies have documented the usefulness of bi-component UTE-T2* analysis for detecting tendon degeneration [9]. Thus, this study was performed to compare bi-component UTE T2* parameters of the patellar tendon between healthy volunteers and patients with patellar tendinopathy to determine whether the quantitative MRI technique could detect changes in the composition and structure of degenerative tendon.

METHODS

Study Group

The study was performed in compliance with Health Insurance Portability and Accountability Act (HIPAA) regulations and with approval from our Institutional Review Board. All subjects signed written informed consent prior to their participation in the study. The study group consisted of 10 healthy volunteers with no prior history of knee pain, injury, or surgery and 11 patients with patellar tendinopathy. All patients with patellar tendinopathy were high-level collegiate or recreational athletes who were diagnosed by a fellowship-trained sports medicine specialist with 15 years of clinical experience (co-author J.J.W.) using standardized criteria which included pain and point tenderness localized to the inferior pole of the patella and load-related anterior knee pain which increased with strenuous use of the knee extensor muscles [13]. The diagnosis of patellar tendinopathy was confirmed on an MRI examination of the knee performed on all patients and interpreted by a fellowship-trained musculoskeletal radiologist with 13 years of clinical experience (co-author R.K.) which showed thickening and increased signal intensity within the patellar tendon and/or absence of any associated findings which could explain an alternative etiology of anterior knee pain.

MRI Examination

An MRI examination was performed on the right knee of all healthy volunteers and the most symptomatic knee of all patients with patellar tendinopathy on the same 3.0T imaging

system (Discovery MR750, GE Healthcare, Waukesha, WI) using an 8-channel phased-array extremity coil (InVivo, Orlando, FL). Foam padding was used to firmly secure the knee within the coil to minimize subject motion during the MRI examination. The knee of all subjects was imaged in the sagittal plane using an intermediate-weighted fast spin-echo sequence with a 2200ms repetition time (TR) and 24ms echo time (TE) and in the sagittal and axial planes using a frequency-selective fat-suppressed T2-weighted fast spin-echo sequence with a 4200ms TR and 85ms TE. Other imaging parameters included a 90° flip angle, 14cm field-of-view, ±31KHz bandwidth, 384×224 in-plane matrix, 3mm slice thickness, and two excitations. The patellar tendon of all subjects was imaged in the sagittal plane using a three-dimensional (3D) gradient-echo-based multi-echo UTE-T2* mapping sequence called 3D-Cones (GE Healthcare, Waukesha, WI) which utilized a k-space sampling scheme of a center-out twisted 3D cone trajectory that allowed a minimal TE of 0.03ms [14]. A total of 16 echoes were acquired at TEs of 0.03, 0.1, 0.8, 1.6, 4.3, 6.0, 8.0, 10.0, 14.0, 16.0, 18.0, 20.0, 24.0, 26.0, 28.0, 30.0ms based upon TE selection from a previous tendon study [3]. For each acquisition, the same TR was used, and four echoes were acquired. Other imaging parameters included a 40ms TR, 20° flip angle, 16cm field-of-view, ±150KHz bandwidth, 256×256 in-plane matrix, 3mm slice thickness, one excitation, 10 slices covering the entire patellar tendon, and 19 minute total scan time. To assess repeatability of bi-component UTE-T2* parameter measurements, 3D-Cones was performed twice on the same knee of the 10 heathy volunteers with the subjects taken out of the scanner and allowed to rest in a sitting position for 10 minutes between scans.

Reconstruction of UTE-T2* Parameter Maps

UTE-T2* parameter maps were created by voxel-by-voxel curve fitting using a custom-made software program based on the non-linear least square "fmincon" function developed in MATLAB (MATLAB 2010b, MathWorks Inc, Natick, MA). All images were registered to the first echo using a rigid registration method implemented in Elastix software to correct for subject motion between scans [15]. A single-component exponential signal model which incorporated Rician noise was used to create 3D parameter maps of single-component UTE-T2* relaxation time (T2*) using an initial parameter guess of T2*= 5ms based on previously published tendon studies and the parameter searching space of [0ms, 100ms] [9, 16]. A bi-component exponential signal model which incorporated Rician noise was used to create 3D parameter maps of the UTE-T2* relaxation times of the fast relaxing macromolecular bound water component ($T2*_F$) and the slow relaxing bulk water component ($T2*_S$) and the fraction of the fast relaxing macromolecular bound water component (F_F) [17]. The initial parameter guess of $T2*_F$= 1ms, $T2*_S$=20ms, and F_F=80% based on previous published tendon studies was used in the iterative optimization [3]. The parameter searching space were [0ms, 20ms], [0ms, 100ms] and [0%, 100%] for $T2*_F$, $T2*_S$, and F_F respectively which reflected a reasonable parameter range for the patellar tendon. The algorithm converging iterations were continued until the step size between the successive estimates was small ($<10^{-8}$), the object function was small ($<10^{-8}$), or total iteration of 1000 was achieved. Voxels which failed the converging iteration criteria or converged at the parameter searching space boundaries were considered outliers and excluded from the parameter maps.

Image Analysis

The patellar tendon of all subjects on all sagittal UTE source images with a TE of 20.0ms, which provided the best morphologic visualization of the tendon, was manually segmented by a research assistant with 6 years of segmentation experience (co-author F.L.) under the supervision of a fellowship-trained musculoskeletal radiologist with 13 years of clinical experience (co-author R.K.) using a custom-made software program developed in MATLAB. The tendon masks were then superimposed over the single-component and bi-component UTE-T2* parameter maps to measure the mean T2*, $T2*_F$, $T2*_S$, and F_F of the entire patellar tendon for all subjects.

The intermediate-weighted and fat-suppressed T2-weighted fast spin-echo sequences and the UTE-T2* parameter maps of all subjects were reviewed by a fellowship-trained musculoskeletal radiologist with 13 years of clinical experience (co-author R.K.). The fast spin-echo images were reviewed to determine the presence of thickening and increased signal intensity within the proximal patellar and to grade the severity of patellar tendinopathy using a previously described grading system (grade 0= clinically diagnosed disease without associated MRI findings of tendon thickening and increased signal intensity, grade 1= increased signal intensity occupying less than 25% of the axial cross-sectional tendon width, grade 2= increased signal intensity occupying between 25% and 50% of the axial cross-sectional tendon width, and grade 3= increased signal intensity occupying more than 50% of the axial cross-sectional tendon width) [18]. The presence of associated knee joint pathology including cartilage loss, bone marrow edema lesions, fat-pad synovitis, fragmentation and edema of the tibia tuberosity, joint effusion, intra-articular body, and tendon, ligament, and meniscus tear was also assessed on the fast spin-echo images. The UTE-T2* parameter maps of all subjects were reviewed to determine the presence of visible changes in $T2*_F$, $T2*_S$, and F_F of the proximal patellar tendon.

Statistical Analysis

Statistical analysis was performed using MATLAB. Statistical significance was defined as a p-value less than 0.05. Wilcoxon rank sum tests were used to compare the mean T2*, $T2*_F$, $T2*_S$, and F_F of the entire patellar tendon between healthy volunteers and patients with patellar tendinopathy. The non-parametric test was best suited for the small number of subjects in our study since it did not require an assumption of normality of the data. The Holm-Bonferroni correction method was used to adjust all *p*-values to account for comparison of multiple UTE-T2* parameters between groups of subjects. Repeatability of tendon UTE-T2* parameter measurements was assessed using coefficient of variation. Bland-Altman analysis was also performed to assess the estimated bias and 95% limits of agreement between the parameter measurements obtained using the two scans. Chi-square statistic was used to assess the quality of fit of the single-component and bi-component exponential signal models. The chi-sqare was first calculated for each voxel volume within the tendon for each subject, and the mean chi-square was then calculated as the average of all voxel-based values within the tendon for all healthy volunteers and patients with patellar tendinopathy [19].

RESULTS

The study group consisted of 10 healthy volunteers (7 males and 3 females with an age range between 22 years and 34 years and an average age of 27.5 years) and 11 patients with patellar tendinopathy (8 males and 3 females with an age range between 19 years and 37 years and average age of 28.1 years). All 10 healthy volunteers showed no knee joint abnormalities on the intermediate-weighted and fat-suppressed T2-weighted fast spin-echo images. Eight patients with patellar tendinopathy showed thickening of the proximal patellar tendon with 7 of these patients also showing increased signal intensity within the proximal patellar tendon on the fast spin-echo images. Two patients with a clinical diagnosis of patellar tendinopathy showed no thickening or increased signal intensity within the patellar tendon. Two patients had grade 0 patellar tendinopathy, 7 patients had grade 1 patellar tendinopathy, and 2 patients had grade 2 patellar tendinopathy. All 11 patients with patellar tendinopathy showed no additional knee joint abnormalities on the fast spin-echo images including patellofemoral compartment cartilage and bone edema lesions, fat pad synovitis, or fragmentation or edema of the tibia which could explain an alternative cause of anterior knee pain.

Mean $T2^*$, $T2^*_F$, $T2^*_S$, and F_F of the entire patellar tendon was 2.0ms (95% confidence intervals 1.5ms to 2.4ms), 1.5ms (95% confidence intervals 1.3ms to 1.8ms), 23.1ms (95% confidence intervals 21.7ms to 25.0ms), and 79.5% (95% confidence intervals 77.8% to 81.4%) respectively for healthy volunteers and 3.1ms (95% confidence intervals 2.8ms to 3.5ms), 1.9ms (95% confidence intervals 1.7ms to 2.1ms), 22.3ms (95% confidence intervals 19.5ms to 24.2ms), and 75.5% (95% confidence intervals 74.7% to 78.9%) respectively for patients with patella tendinopathy. Patients with patellar tendinopathy had significantly higher $T2^*$ (p=0.001) and $T2^*_F$ (p=0.01) and significantly lower F_F (p=0.007) of the patellar tendon when compared to healthy volunteers. There was no significant difference (p=0.10) in $T2^*_S$ of the patellar tendon between healthy volunteers and patients with patellar tendinopathy.

Figure 1a shows sagittal images through the patellar tendon in a healthy volunteer at all 16 echoes acquired using the 3D-Cone UTE-T2* mapping sequence. There was a monotonic decay of the MRI signal of the patellar tendon with much stronger decay occurring prior to 4.3ms than after 4.3ms. Figure 1b and 1c shows signal intensity curves for a region of interest placed in the patellar tendon in a healthy volunteer and a patient with patellar tendinopathy respectively. There was visibly improved curve fit of the signal intensity values when using a bi-component exponential signal model. The mean chi-square was lower for the bi-component exponential signal model (146 and 156 for healthy volunteers and patients with patellar tendinopathy respectively) than for the single-component exponential signal model (284 and 320 for healthy volunteers and patients with patellar tendinopathy respectively) confirming a better quality of fit when using the bi-component model.

Figures 2 and 3 illustrate examples of differences in UTE-T2* parameter maps of the patellar tendon between healthy volunteers and patients with grades 0 and grade 2 patellar tendinopathy respectively. All patients with patellar tendinopathy, including the 2 patients with grade 0 tendinopathy, showed focal areas of visibly increased $T2^*_F$ and decreased F_F in

the proximal patellar tendon. No healthy volunteers showed visible changes in the patellar tendon on the UTE-T2* parameter maps.

Coefficients of variation for repeat UTE-T2* parameter measurements of the patellar tendon from 3D-Cones scans performed twice on the same knee of the 10 healthy volunteers were 3.8% for $T2*_F$, 4.8% for $T2*_S$, and 2.4% for F_F. The estimated bias for repeat parameter measurements on Bland-Altman analysis were 0.01ms for $T2*_F$, −0.2ms for $T2*_S$, and 2.2% for F_F, while the 95% limits of agreement were −0.17ms to 0.19ms for $T2*_F$, −4.8ms to 4.4ms for $T2*_S$, and −4.2% to 8.5% for F_F.

DISCUSSION

Our study found that patients with patellar tendinopathy had significantly higher $T2*_F$ and significantly lower F_F of patellar tendon when compared to healthy volunteers. Juras and associates also investigated the use of bi-component UTE-T2* parameters for detecting tendon degeneration and found that patients with Achilles tendinopathy had significantly higher $T2*_F$ but similar $T2*_S$ and F_F when compared to healthy volunteers [9]. However, the UTE-T2* mapping sequence used in this study had a minimum echo time of 0.8ms and acquired only a limited number of short echoes to assess the fast relaxing water component of tendon. This was likely the cause of the decreased sensitivity of F_F for detecting tendon degeneration and the lower measured F_F values of both healthy and diseased tendon in the study performed by Juras and associates when compared to our study [9].

Tendon consists primarily of highly ordered type 1 collagen fibers embedded in a ground substance comprised of water, proteoglycan, glycoproteins, and other small molecules [20]. Tendon degeneration results in decrease in collagen content, increase in water, proteoglycan and lipid content, and collagen disorganization on both the microstructural (i.e. triple helical tropocollagen and fibril) and macrostructural (i.e. fiber and fascicular) level [8]. The fundamental mechanisms responsible for changes in F_F, $T2*_F$, and $T2*_S$ in patients with patellar tendinopathy are purely speculative as no previous studies have correlated bi-component UTE-T2* parameters with biochemical or microstructural properties of normal or diseased tendon. However, the lower F_F in patients with patellar tendinopathy may be due to decrease in collagen content and increase in bulk water content of degenerated tendon. The higher $T2*_F$ in patients with tendinopathy may be the result of collagen fiber disruption on the microstructural level which results in decreased restriction of collagen bound water. Disruption and disorganization of collagen at the macrostructural level would theoretically result in decreased restriction of bulk water within tendon and thus lead to an increase in $T2*_S$. However, our study and the study performed by Juras and associates [9] found no significant difference in $T2*_S$ between patients with tendinopathy and healthy volunteers. This may be the result of the increased uncertainty and higher sensitivity to noise of $T2*_S$ parameter estimation due to the relatively small fraction of the slow relaxing water component in tendon which provides little MRI signal at later echoes [21].

Single component UTE-T2* mapping techniques have been previously used to detect tendon degeneration and have shorter scan times and less complex reconstruction algorithms when compared to bi-component UTE-T2* mapping techniques [7]. In fact, our study found that

patients with patellar tendinopathy had significantly higher T2* when compared to healthy volunteers. However, bi-component UTE-T2* analysis of tendon has many potential advantages when compared to single-component UTE-T2* analysis. Our study and other recently published studies have demonstrated that bi-component exponential signal models are better suited than single-component models for evaluating tendon with improved quality of curve fitting [3, 9–11]. Juras and associates compared single-component and bi-component UTE-T2* analysis of the Achilles tendon in human subjects and found that the bi-component analysis provided greater diagnostic performance for distinguishing between healthy and diseased tendon [9]. Bi-component UTE-T2* analysis may also be useful for monitoring disease-related and treatment-related changes in tendon composition and structure. For example, F_F may be useful for detecting changes in the collagen and bulk water content of tendon, while $T2^*_F$ and $T2^*_S$ may be useful for detecting changes in collagen organization on both the microstructural and macrostructural levels respectively.

Our study has several limitations. First, our study focused exclusively on the patellar tendon and included only a relatively small number of healthy volunteers and patients with patellar tendinopathy. In particular, the small number of subjects did not allow us to investigate potential differences in $T2^*_F$, $T2^*_S$, and F_F between patients with different grades of patellar tendinopathy and to determine the association between bi-component UTE-T2* parameters and the severity of knee pain and functional disability in patients with patellar tendinopathy. Furthermore, our study did not investigate the mechanisms responsible for differences in bi-component UTE-T2* parameters between healthy volunteers and patients with patellar tendinopathy. Additional studies correlating F_F, $T2^*_F$, and T2* in ex-vivo patellar tendon specimens with collagen, water, proteoglycan, and lipid content using biochemical assays and collagen microstructure and macrostructure using conventional and polarized light microscopy are needed to investigate the factors responsible for changes in bi-component UTE-T2* parameters at various stages of tendon degeneration.

In conclusion, our study has shown that bi-component UTE-T2* parameters measured using 3D-Cones can detect changes in the composition and structure of degenerated tendon in patients with patellar tendinopathy. The 3D-Cones UTE-T2* mapping sequence used in our study provided complete anatomic coverage of the patellar tendon in a clinically feasible scan time on a 3.0T imaging system and had high repeatability for measuring bi-component UTE-T2* parameters with coefficients of variation which compared favorably with other quantitative musculoskeletal MRI techniques [22–24]. 3D-Cones may provide a new quantitative MRI method to identify patients with early tendon degeneration in clinical practice and to monitor disease-related and treatment-related changes in tendon composition and structure in longitudinal research studies. However, further studies are needed to better understand the fundamental mechanisms responsible for changes in F_F, $T2^*_F$, and T2* in patients with patellar tendinopathy and other tendon disorders and to investigate the responsiveness of bi-component UTE-T2* parameters to changes in tendon degeneration and tendon healing following therapy.

Acknowledgments

References

1. Chang EY, Du J, Chung CB. UTE imaging in the musculoskeletal system. Journal of magnetic resonance imaging: JMRI. 2015; 41:870–883. [PubMed: 25045018]

2. Koff MF, Pownder SL, Shah PH, Yang LW, Potter HG. Ultrashort echo imaging of cyclically loaded rabbit patellar tendon. Journal of biomechanics. 2014; 47:3428–3432. [PubMed: 25234349]

3. Chang EY, Du J, Iwasaki K, Biswas R, Statum S, He Q, Bae WC, Chung CB. Single- and Bi-component T2* analysis of tendon before and during tensile loading, using UTE sequences. Journal of magnetic resonance imaging: JMRI. 2015; 42:114–120. [PubMed: 25223714]

4. Chang EY, Bae WC, Statum S, Du J, Chung CB. Effects of repetitive freeze-thawing cycles on T2 and T2 of the Achilles tendon. European journal of radiology. 2014; 83:349–353. [PubMed: 24239237]

5. Chang EY, Du J, Bae WC, Statum S, Chung CB. Effects of Achilles tendon immersion in saline and perfluorochemicals on T2 and T2*. Journal of magnetic resonance imaging: JMRI. 2014; 40:496–500. [PubMed: 24155129]

6. Grosse U, Springer F, Hein T, Grozinger G, Schabel C, Martirosian P, Schick F, Syha R. Influence of physical activity on T1 and T2* relaxation times of healthy Achilles tendons at 3T. Journal of magnetic resonance imaging: JMRI. 2015; 41:193–201. [PubMed: 24347267]

7. Grosse U, Syha R, Hein T, Gatidis S, Grozinger G, Schabel C, Martirosian P, Schick F, Springer F. Diagnostic value of T1 and T2 * relaxation times and off-resonance saturation effects in the evaluation of Achilles tendinopathy by MRI at 3T. Journal of magnetic resonance imaging: JMRI. 2015; 41:964–973. [PubMed: 24817378]

8. Xu Y, Murrell GA. The basic science of tendinopathy. Clinical orthopaedics and related research. 2008; 466:1528–1538. [PubMed: 18478310]

9. Juras V, Apprich S, Szomolanyi P, Bieri O, Deligianni X, Trattnig S. Bi-exponential T2 analysis of healthy and diseased Achilles tendons: an in vivo preliminary magnetic resonance study and correlation with clinical score. European radiology. 2013; 23:2814–2822. [PubMed: 23760303]

10. Chang EY, Du J, Statum S, Pauli C, Chung CB. Quantitative bi-component T2* analysis of histologically normal Achilles tendons. Muscles Ligaments Tendons J. 2015; 5:58–62. [PubMed: 26261782]

11. Diaz E, Chung CB, Bae WC, Statum S, Znamirowski R, Bydder GM, Du J. Ultrashort echo time spectroscopic imaging (UTESI): an efficient method for quantifying bound and free water. NMR Biomed. 2012; 25:161–168. [PubMed: 21766381]

12. Juras V, Zbyn S, Pressl C, Valkovic L, Szomolanyi P, Frollo I, Trattnig S. Regional variations of T(2)* in healthy and pathologic achilles tendon in vivo at 7 Tesla: preliminary results. Magnetic resonance in medicine: official journal of the Society of Magnetic Resonance in Medicine/Society of Magnetic Resonance in Medicine. 2012; 68:1607–1613.

13. Lian OB, Engebretsen L, Bahr R. Prevalence of jumper's knee among elite athletes from different sports: a cross-sectional study. The American journal of sports medicine. 2005; 33:561–567. [PubMed: 15722279]

14. Gurney PT, Hargreaves BA, Nishimura DG. Design and analysis of a practical 3D cones trajectory. Magn Reson Med. 2006; 55:575–582. [PubMed: 16450366]

15. Klein S, Staring M, Murphy K, Viergever MA, Pluim JP. elastix: a toolbox for intensity-based medical image registration. IEEE Trans Med Imaging. 2010; 29:196–205. [PubMed: 19923044]

16. Raya JG, Dietrich O, Horng A, Weber J, Reiser MF, Glaser C. T2 measurement in articular cartilage: impact of the fitting method on accuracy and precision at low SNR. Magnetic resonance in medicine: official journal of the Society of Magnetic Resonance in Medicine/Society of Magnetic Resonance in Medicine. 2010; 63:181–193.

17. Gudbjartsson H, Patz S. The Rician distribution of noisy MRI data. Magn Reson Med. 1995; 34:910–914. [PubMed: 8598820]

18. Johnson DP, Wakeley CJ, Watt I. Magnetic resonance imaging of patellar tendonitis. The Journal of bone and joint surgery British volume. 1996; 78:452–457. [PubMed: 8636185]

19. Bouhrara M, Reiter DA, Celik H, Bonny JM, Lukas V, Fishbein KW, Spencer RG. Incorporation of rician noise in the analysis of biexponential transverse relaxation in cartilage using a multiple gradient echo sequence at 3 and 7 tesla. Magn Reson Med. 2015; 73:352–366. [PubMed: 24677270]

20. Kannus P. Structure of the tendon connective tissue. Scandinavian journal of medicine & science in sports. 2000; 10:312–320. [PubMed: 11085557]

21. Liu F, Kijowski R. Assessment of different fitting methods for in-vivo bi-component T2* analysis of human patellar tendon at 3.0T. Muscles Ligaments Tendons J. (In Press).

22. Multanen J, Rauvala E, Lammentausta E, Ojala R, Kiviranta I, Hakkinen A, Nieminen MT, Heinonen A. Reproducibility of imaging human knee cartilage by delayed gadolinium-enhanced MRI of cartilage (dGEMRIC) at 1.5 Tesla, Osteoarthritis and cartilage/OARS. Osteoarthritis Research Society. 2009; 17:559–564.

23. Glaser C, Mendlik T, Dinges J, Weber J, Stahl R, Trumm C, Reiser M. Global and regional reproducibility of T2 relaxation time measurements in human patellar cartilage. Magnetic resonance in medicine: official journal of the Society of Magnetic Resonance in Medicine/Society of Magnetic Resonance in Medicine. 2006; 56:527–534.

24. Mosher TJ, Zhang Z, Reddy R, Boudhar S, Milestone BN, Morrison WB, Kwoh CK, Eckstein F, Witschey WR, Borthakur A. Knee articular cartilage damage in osteoarthritis: analysis of MR image biomarker reproducibility in ACRIN-PA 4001 multicenter trial. Radiology. 2011; 258:832–842. [PubMed: 21212364]
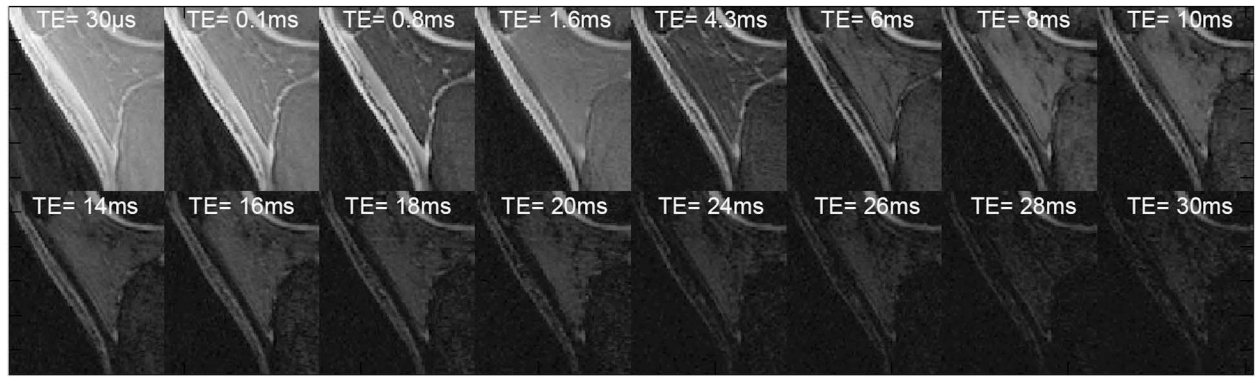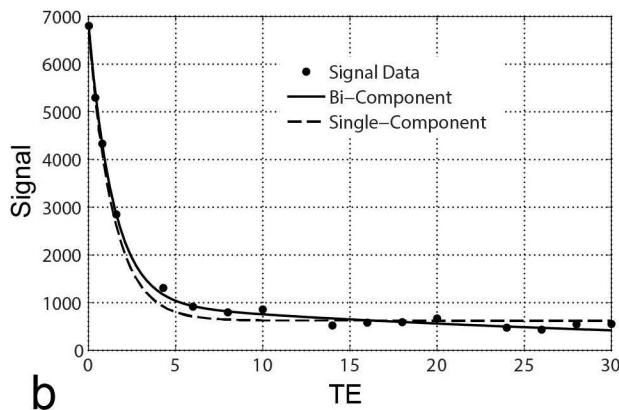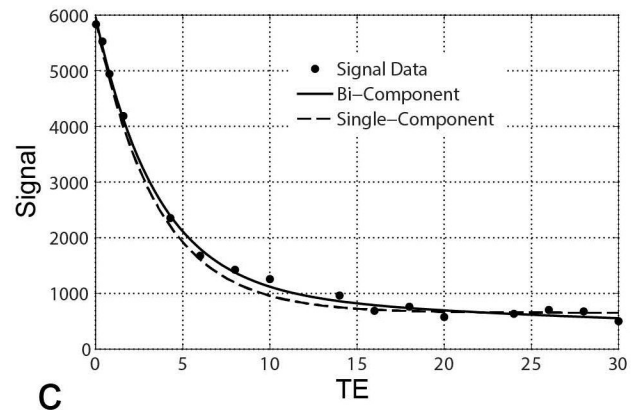
Figure 1.
(a) Sagittal images through the patellar tendon in a 27 year old healthy male volunteer at all 16 echoes acquired using the 3D-Cones UTE-T2* mapping sequence. Note that there is little MRI signal remaining in the patellar tendon on images with TEs of 4.3ms and longer. (b and c) Signal intensity curves for a homogenous region of interest placed in a sagittal image through the central patellar tendon in a 27 year old healthy volunteer and a 21 year old patient with patellar tendinopathy respectively. Note that there is visibly improved curve fit of the signal intensity values when using a bi-component exponential signal model.
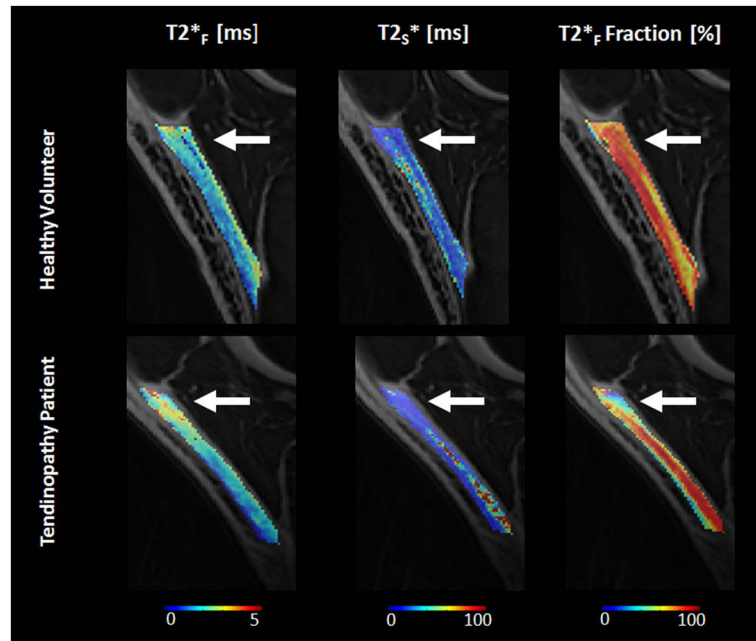
Figure 2.
UTE-T2* parameter maps in a 25 year old healthy male volunteer and a 21 year old high-level collegiate male basketball player with grade 0 patellar tendinopathy (i.e. clinically diagnosed disease without associated MRI findings of tendon thickening and increased signal intensity). Note the small focal area of increased $T2_F$ and decreased F_F in the proximal patellar tendon in the patient with patellar tendinopathy with no visible change in $T2_S$ (arrows).
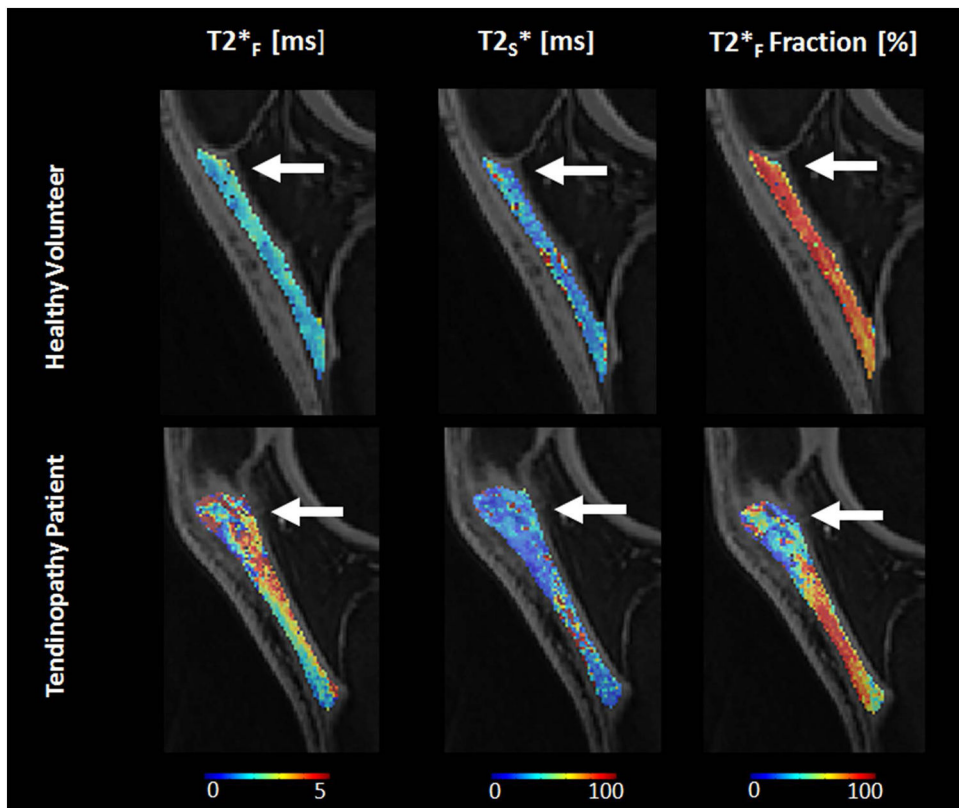
Figure 3.
UTE-T2* parameter maps in a 27 year old healthy male volunteer and 32 year old high-level recreational male runner and volleyball player with grade 2 patellar tendinopathy (i.e. increased signal intensity between 25% and 50% of the axial cross-sectional tendon width). Note the large focal area of increased $T2_F$ and decreased F_F in the proximal patellar tendon in the patient with patellar tendinopathy with no visible change in $T2_S$ (arrows).